Implementation of a New Assimilation Scheme for Soil and Surface Variables in a Global NWP Model

D. GIARD AND E. BAZILE

Météo-France/CNRM, Toulouse, France

(Manuscript received 27 July 1998, in final form 26 May 1999)

ABSTRACT

Major changes have been introduced in the description of the soil–atmosphere–vegetation interactions in the global numerical weather prediction model ARPEGE and the embedded limited area model ALADIN used at Météo-France. The Interaction Soil Biosphere Atmosphere (ISBA) parameterization is now used to describe exchanges between the atmosphere and the land surface. The analysis scheme for soil moisture has been changed accordingly and is now based on an optimal interpolation type using 2-m observations of temperature and relative humidity. Additionally, the description of land surface and vegetation characteristics has been improved by the use of new datasets. The overall impact of these modifications is a clear improvement in the forecast of low-level fields and of the global hydrological cycle.

1. Introduction

While most operational numerical weather prediction (NWP) models, following general circulation models, are moving toward more sophisticated land surface parameterizations (e.g., Viterbo and Beljaars 1995; Cox 1996), the one used until recently in the operational suite at Météo-France remained very simple. In this former configuration, two thin adjacent soil layers were considered for temperature and moisture. Vegetation was taken into account only through a slight modification of evaporation. A simple analysis scheme for soil variables was also implemented. Observations of 2-m temperature (T_{2m}) and 2-m relative humidity (H_{2m}) were used to correct, respectively, soil temperature and soil moisture (Urban et al. 1985; Coiffier et al. 1987). To avoid strong diurnal oscillations of soil moisture, a recursive filtering acting on relative humidity had to be introduced at a later stage. An additional relaxation toward climatology for all surface and soil variables also acted to prevent long-term drifts with respect to the annual cycle inside the data assimilation procedure.

In the meantime, a new land surface parameterization was developed at Météo-France, the so-called Interaction Soil Biosphere Atmosphere (ISBA) scheme (Noilhan and Planton 1989; Noilhan and Mahfouf 1996). It has been extensively tested against field experiments (see Noilhan and Mahfouf 1996 for a short review) and behaves reasonably well in international comparison projects, as shown in Henderson-Sellers et al. (1995) for instance. Recently, it has also been successfully coupled with hydrological models (Habets et al. 1999). Implemented first in 1D or mesoscale models (Bougeault et al. 1991) for research purposes, ISBA was later used, in a slightly different version, for low-resolution climate runs (Manzi and Planton 1994). The next step was its implementation in the French NWP models—the global variable resolution model ARPEGE (Action de Recherche Petite Echelle Grande Echelle), and the embedded limited area model ALADIN (Aire Limitée Adaptation Dynamique Développement International)—an action that is the central topic of the present paper.

Apart from some further developments or tunings, described in section 3 and required to face problems encountered in the context of NWP, this operational change implied the design of a new analysis scheme to initialize the superficial and mean soil temperature and moisture consistently with ISBA. Some preliminary sensitivity experiments, based on 72-h forecasts, were performed to appraise the importance of soil moisture analysis with the new surface scheme (Bazile and Giard 1996). They showed that errors in the initial soil water content can lead to quite large changes in the forecast of T_{2m} and H_{2m}, up to 4 K and 0.50, respectively. Though already used in the French operational NWP models for years (Coiffier et al. 1987), assimilation of soil and surface variables, especially moisture, was focused upon more recently. Mahfouf (1991) studies the feasibility of soil moisture analysis from observations of T_{2m} and H_{2m}

Corresponding author address: Dr. Dominique Giard, Météo-France, CNRM-GMAP, 42, Avenue Coriolis, F-31057 Toulouse Cedex, France.
E-mail: dominique.giard@meteo.fr

using ISBA in a 1D mode. Both variational and optimal interpolation (OI) methods are considered, and the corresponding statistics are derived using a Monte Carlo method for a discrete set of soil and vegetation characteristics. Bouttier et al. (1993a,b) go further with sequential OI analyses of surface and deep soil water contents. They made an attempt at an analytical formulation for the OI coefficients computed by Mahfouf (1991) and academic tests in a mesoscale model for a well-documented and predicted situation. More recently, the European Centre for Medium-Range Weather Forecasts model had to face problems related to large drifts of soil moisture, finally solved with the implementation of a very simple correction scheme. The soil moisture corrections are derived from analysis increments for specific humidity at the lowest model level (Viterbo and Courtier 1995). Soil and surface temperatures are not analyzed, and observations of T_{2m} are not used in this case.

Some other assimilation schemes for soil moisture or soil temperature, using remotely sensed observations (van den Hurk et al. 1997) or based on variational analysis (Callies et al. 1998; Bouyssel et al. 1998), are currently being studied but are likely to be used operationally only on a longer-term basis. What was decided for ARPEGE was to use sequential analysis from observations of T_{2m} and H_{2m} for surface and soil moisture, following Mahfouf (1991) and using the OI-type coefficients already computed for ISBA. The operational soil temperature analysis, as described in Coiffier et al. (1987), was kept unchanged, even if the ISBA predictive equation for these variables is more sophisticated than the previously used one. The main features of the assimilation procedure are described in section 4.

The last aspect of the implementation, described hereafter, is the improvement in the description of the land surface in the model. It is all the more important since the sensitivity to soil and vegetation characteristics increases as more detailed parameterizations or analysis schemes are used. The overall impact of these changes, assessed through a one-year-long assimilation suite at low resolution and two parallel suites in quasi-operational configuration, are presented in section 5.

2. Description of the land surface

ARPEGE is a global spectral variable mesh model (Courtier and Geleyn 1988) with enhanced resolution over Europe. For the operational configuration, a triangular truncation T199 with a stretching factor (c) equal to 3.5 and a quadratic-type Gaussian grid, the grid size ranges from 20 km over France to 240 km at the antipodes. However, the experiments described hereafter, performed with the global model, used lower resolutions: T119c3.5 for sensitivity tests and tunings over two periods (sections 2–4), T149c3.5 for parallel runs (section 5). These are the operational configurations until October 1995 and September 1998, respectively. The corresponding resolutions are described in Table 1. For the several operational versions of ALADIN (Members of the ALADIN International Team 1997), covering Europe and Northern Africa, resolution lies between 7 and 17 km, but it can be smaller for research purposes, e.g., nonhydrostatic experiments. As a consequence, not only global datasets, but also local high-resolution ones covering at least Europe, are required to define soil and vegetation characteristics.

TABLE 1. Characteristics of the various truncations used for the ARPEGE model.

Trunctation	Stretching factor	Grid points	Max resolution (over France in km)	Min resolution (over New Zealand in km)
T79	$c = 1$	240 × 120	160	160
T119	$c = 3.5$	360 × 180	32	390
T149	$c = 3.5$	448 × 224	26	315
T199	$c = 3.5$	600 × 300	20	240

The soil characteristics required for ISBA are the useful soil depth (d_p), combining the hydrological depth and the rooting depth (d_r), and the corresponding fractions of sand and clay, used to describe soil texture following Giordani (1993). The International Satellite Land Surface Climatology Project Initiative 1 dataset (Sellers et al. 1996) has been used for hydrological soil depth, whereas texture is derived from Webb et al. (1991). Both datasets are global with a resolution of 1° and consistent with each other. The rooting depth has been derived from land cover maps.

Three fields are explicitly used to describe the vegetation in ISBA: the vegetation fraction (veg), the leaf area index (LAI), and the minimum surface resistance ($R_{\rm sm}$). A land use index is also required to discriminate between sea/lake, glacier, desert/low vegetation, and forest in the evaluation of the thermal inertia coefficients or the contribution of photosynthesis to surface resistance (Noilhan and Planton 1989). The contribution of vegetation to the soil depth, the roughness length, and the albedo (d_r, $z0_v$, α_v) must also be evaluated.

Two different land cover maps and the corresponding lookup tables have been used as described in Champeaux et al. (1999). First, a global coverage is obtained with the Wilson and Henderson-Sellers (1985) data, at a resolution of 1°, using an aggregation of classes and lookup tables (appendix A) as described in Mahfouf et al. (1995). Afterward, vegetation characteristics are modified over Europe using a preliminary version of the Champeaux database, derived from National Oceanic and Atmospheric Administration's Advanced Very High Resolution Radiometer observations (Champeaux and Le Gléau 1995; Champeaux et al. 1999). It provides an improved resolution, with a 2-km mesh size, a reliable forest mask, and a more accurate description of the annual cycle of vegetation, with the distinction between several types of crops (appendix B).

Ten-day long assimilation experiments have been performed to evaluate the impact of these new high-resolution data with respect to the global dataset, over a summer (July 1995) and a winter (January 1995) situation. The largest differences in the description of vegetation lie over Spain in July. Using the new data the mean values of veg and LAI decrease from 0.83 to 0.53 and from 2.9 to 1.5 $m^2\ m^{-2}$, respectively, and the forecast of T_{2m} and H_{2m} is improved as shown in Fig. 1. When averaged over Spain and over 10 days, the gain is about 0.5 K and 0.05, respectively, but it can be much higher locally, as much as 1 K and 0.15. The evolution of soil moisture and the value of the Bowen ratio are simultaneously improved. The sensitivity to soil texture has also been tested, through 72-h forecast experiments, and remains small at the scale considered here.

3. Modifications to the land surface scheme

Moving to operational NWP is a difficult test for any parameterization. Whereas feedback effects with dynamics and the rest of parameterization schemes may be important and a very large range of situations is to be considered, checkings are very strict, with a continuous verification against observations as well as a control of global balances. Such constraints are even stronger in a global variable resolution model. As a consequence, some necessary refinements were brought to the ISBA scheme, while some options requiring further validation were not introduced in the present operational version. With respect to the most up-to-date reference paper for ISBA (Noilhan and Mahfouf 1996), the differences are the following:

- the ratio of dynamical to thermal roughness length is constant, equal to 10 over land and 1 over sea, and the computation of exchange coefficients is slightly modified in order to recover the previous values in the limiting case of equal lengths;
- the thermal inertia coefficient C_t, controling the diurnal cycle of surface temperature, is limited to low values;
- the formulation of the hydric coefficient C_1, involved in the evolution of superficial soil moisture, has been improved for very dry soils as described hereafter;
- a parameterization of soil water freezing has been added and another prognostic variable, the total frozen soil water content (W_f), had therefore to be introduced.

The resulting prognostic equations for the six surface variables—the surface temperature (T_s), the mean soil temperature (T_p), the interception water content (W_l), the superficial (liquid) soil water content (W_s) or the superficial volumetric water content (ω_s, $W_s = \rho d_s \omega_s$), the total liquid soil water content (W_p) or the mean volumetric water content (ω_p, $W_p = \rho d_p \omega_p$), and W_f—are as follows:

$$\frac{\partial T_s}{\partial t} = \underline{C_t}[R_n - H - L_v(E_g + E_l + E_{\rm tr}) - L_f(M_s - \underline{F_w})] - \frac{2\pi}{\tau}(T_s - T_p), \quad (1)$$

$$\frac{\partial T_p}{\partial t} = \frac{(T_s - T_p)}{\tau}, \quad (2)$$

$$\frac{\partial W_l}{\partial t} = \text{veg} \cdot P - E_l - R_l, \quad (3)$$

$$\rho d_s \frac{\partial \omega_s}{\partial t} = \underline{C_1}[(1 - \text{veg}) \cdot P - E_g + R_l + M_s] - \rho d_s \frac{C_2}{\tau} \cdot (\omega_s - \omega_{\rm seq}) - R_s, \quad (4)$$

$$\rho d_p \frac{\partial \omega_p}{\partial t} = (1 - \text{veg}) \cdot P - E_g - E_{\rm tr} + R_l + M_s - \underline{F_w} - R_p - \rho d_p \frac{C_3}{\tau} \cdot (\omega_p - \omega_{\rm fc}), \quad \text{and} \quad (5)$$

$$\underline{\frac{\partial W_f}{\partial t} = F_w}. \quad (6)$$

The new or modified terms are underlined. Notations are specified in appendix C and the formulation of fluxes follows Noilhan and Mahfouf (1996), for those not detailed hereafter.

The thermal inertia coefficient C_t now reads

$$C_t = \left[\frac{(1 - \text{veg})(1 - f)}{C_g} + \frac{(1 - \text{veg})f}{C_i} + \frac{\text{veg}}{C_v}\right]^{-1}, \quad (7)$$

where $f = W_f(W_p + W_f)^{-1}$ is the fraction of frozen water in the soil, C_v is the thermal inertia coefficient for the canopy, $C_i = 5.6 \times 10^{-6}$ K m^2 J^{-1} is for the soil ice, and C_g is for the soil:

$$C_g = \min\left\{C_{g_{\max}}, C_{g_{\rm sat}}\left[\frac{\omega_{\rm sat}}{\max(\omega_p, \omega_{\rm wilt})}\right]^{(b/\log 10)}\right\}. \quad (8)$$

Here, b depends on soil texture (Noilhan and Planton 1989), and C_g is limited to its value at wilting point, with a maximum $C_{g_{\max}}$ set to 8×10^{-6} K m^2 J^{-1}. This constraint is also applied to C_v, which corresponds to a strong reduction when compared to 10^{-3} K m^2 J^{-1} in Noilhan and Planton (1989) or 2×10^{-5} K m^2 J^{-1} in Noilhan and Mahfouf (1996), but still remains in agreement with calibrations for low vegetation (Calvet et al. 1998). These limitations are required for a better representation of the diurnal cycle of surface and low-level atmospheric variables, particularly to reduce cold (for T_{2m}) and wet (for H_{2m}) biases during night (Giard and Bazile 1996, 1997b). A consequence is a very narrow range of variation for C_g and C_t, since the minimum value ($C_{g_{\rm sat}}$) stays between 3×10^{-6} and 4.5×10^{-6} K m^2 J^{-1} and ω_p lies far below saturation (Noilhan and

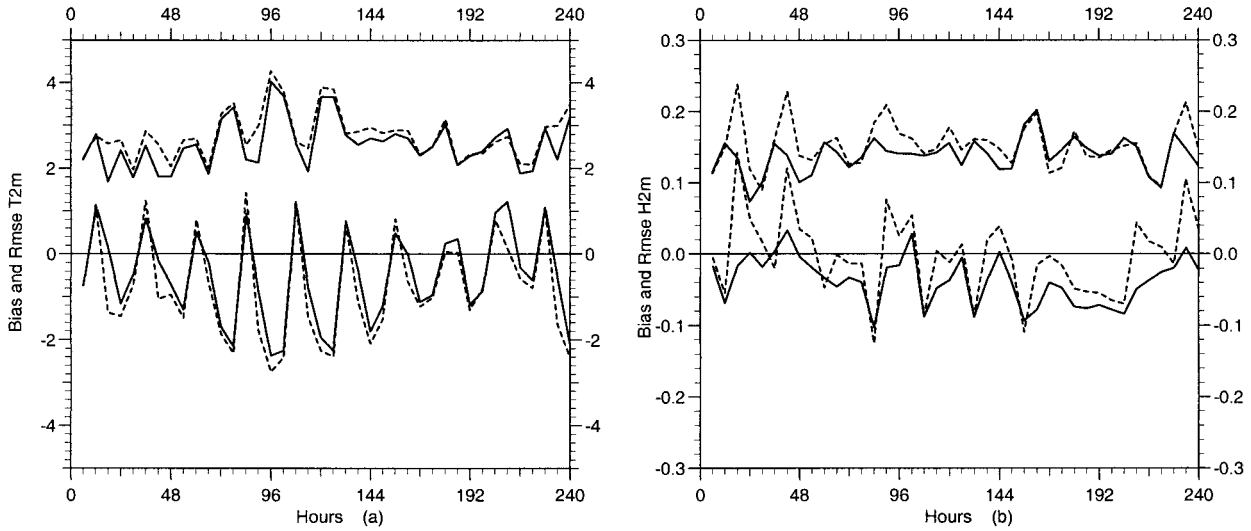

FIG. 1. Difference between predicted and observed (SYNOP) values (mean and rms errors) during 10-day long assimilation experiments from 2 July 1995, over Spain (36°N, 10°W; 44°N, 0°): (a) T_{2m}, (b) H_{2m}. Full line: new high-resolution vegetation. Dashed line: old vegetation (model − obs. is plotted).

Planton 1989). Since the surface parameterization is not the only determining process in such problems, this constraint may be alleviated later with further improvements in the rest of the physics.

The formulation of the hydric coefficient C_1 is close to that of Noilhan and Mahfouf (1996):

$$C_1 = \begin{cases} C_{1\max} d_s \exp[-(\omega_s - \omega_{\max})^2/\sigma] & \text{for } \omega_s < \omega_{\text{wilt}} \\ C_{1\text{sat}} d_s (\omega_{\text{sat}}/\omega_s)^{(b/2+1)} & \text{for } \omega_s \geq \omega_{\text{wilt}}, \end{cases}$$

where $C_{1\max}$ is computed as previously from ω_{wilt} and T_s. The position ($\omega_{\max}$) and the width (σ) of the Gaussian shape are adjusted locally so as to ensure continuity of the formulation at the wilting point (a constraint that was not always satisfied with the previous formulas) and to fix a minimum value for very dry soils: $C_1(0) = 0.1$ (Giard and Bazile 1996, 1997b). This improves the description of the diurnal cycle, by a reduction of warm and dry biases around midday, as expected from Braud et al. (1993) for dry soils, but also avoids problems with very dry soils, where spurious cold and wet biases may result from very low values of C_1 (Giard and Bazile 1996, 1997b).

The last modification has been the introduction of a parameterization of soil water freezing in the ISBA scheme (Bazile and Giard 1998). The soil water freezing rate F_w results from the contributions of melting (F_m) and freezing (F_f) as follows:

$$F_w = F_f - F_m, \tag{9}$$

$$F_f = K\left(\frac{W_p - W_s}{\rho d_p \omega_{\text{sat}}}\right) \max(0,\, T_t - T^*), \quad \text{and} \tag{10}$$

$$F_m = K \max(0,\, T_s - T_t). \tag{11}$$

Freezing occurs below the triple point T_t, once the cooling effect of snow melting on T_s is introduced. A combination (T^*) of the modified surface temperature (T_s^+) and mean soil temperature T_p is used to take into account the insulating role of snow: $T^* = T_s^+(1 - S_n) + T_p \cdot S_n$, where S_n is the snow cover fraction. The soil water freezing rate (F_f) increases following the available soil moisture, excluding the superficial layer, and is limited: $W_f \leq W_{f_{\max}}$. On the other hand, above the triple point, melting depends only on the surface temperature. A dependency on vegetation characteristics has also been introduced to parameterize the insulating effect of the canopy, through the formulation of the melting coefficient K:

$$K = \left(1 - \frac{\text{veg}}{K_2}\right)\left(1 - \frac{\text{LAI}}{K_3}\right) \Big/ (C_i L_f \tau_w). \tag{12}$$

The following set of constants has been tuned to fit the observations in 1D experiments with various types of vegetation (bare ground, forest, and low vegetation): $\tau_w = 4500$ s, $K_1 = 5$, $K_2 = 30$. Figure 2 illustrates the impact of this parameterization. Two 24-h forecasts, with and without soil water freezing, have been performed using the 1D version of ARPEGE. Initial fields are extracted from a full ARPEGE forecast, at a grid point near the SYNOP station Francazal (France, 43.52°N, 1.31°E). A cold winter situation (2 January 1995) is chosen, starting from 1800 UTC. The predicted 2-m temperature and the corresponding observations are plotted. The modification avoids spurious cooling during the night (by about 2 K at dawn) and enables a better fit to observations. Parallel suites have also confirmed the improvement in the forecast of minimum temperatures for cold situations.

Since assimilation of soil moisture is of concern here,

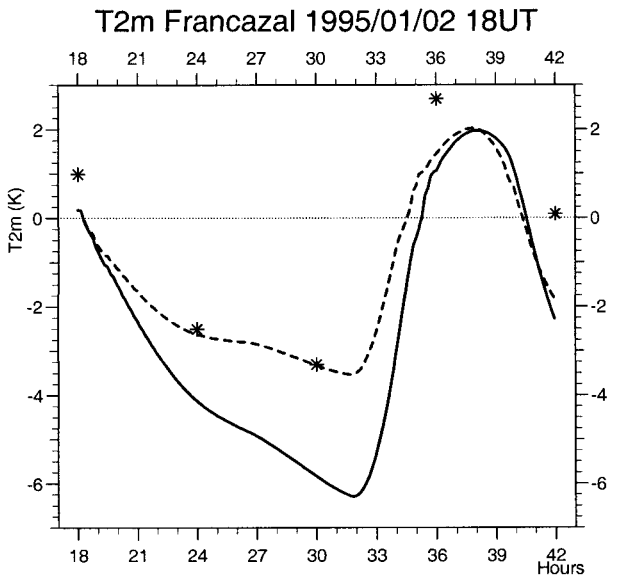

FIG. 2. Time evolution of T_{2m} from 2 Jan 1995 at 1800 UTC to 3 Jan 1995 at 1800 UTC. Stars: observations. Full line: ISBA. Dashed line: ISBA with soil water freezing.

its impact on surface fluxes within the ISBA scheme is to be underlined. The superficial soil moisture (i.e., ω_s) controls bare-ground evaporation E_g via the surface relative humidity H_s:

$$E_g = (1 - \text{veg})\rho_a C_H V_a [H_s q_{\text{sat}}(T_s) - q_a] \quad \text{and} \tag{13}$$

$$H_s = \max\left\{\sin^2\left[\frac{\pi}{2}\min\left(1, \frac{\omega_s}{\omega_{\text{fc}}}\right)\right], \min\left[1, \frac{q_a}{q_{\text{sat}}(T_s)}\right]\right\} \times (1 - S_n) + S_n. \tag{14}$$

Its influence tends to vanish as the vegetation or snow cover widens, or in case of dew or rain ($E_g \leq 0$), and sensitivity is lost above field capacity (ω_{fc}). The mean soil moisture (i.e., ω_p) drives bare-ground evaporation through a very strong control on ω_s [via ω_{seq} in Eq. (4)]. It has an impact on the diurnal cycle of surface temperature and the related fluxes via the bare-ground component of the soil thermal inertia, though reduced by the above modifications. Its last contribution is to transpiration E_{tr} through the surface resistance R_s:

$$E_{\text{tr}} = \text{veg}\frac{\rho_a}{R_a + R_s}(1 - \delta)[q_{\text{sat}}(T_s) - q_a], \quad \text{with}$$

$$R_a = (C_H V_a)^{-1}, \quad \text{and} \quad \delta = \left(\frac{W_l}{W_{l\max}}\right)^{2/3}; \tag{15}$$

$$\frac{1}{R_s} = \frac{\text{LAI}}{R_{\text{sm}}}\max\left[0, \min\left(1, \frac{\omega_p - \omega_{\text{wilt}}}{\omega_{\text{fc}} - \omega_{\text{wilt}}}\right)\right]\frac{F_3 F_4}{F_1}. \tag{16}$$

The functions F_1, F_3, F_4, and $W_{l\max}$ are detailed in Noilhan and Planton (1989). Transpiration decreases as the vegetation cover becomes more sparse, roughly when either veg or LAI/R_{sm} tend toward 0, or as the fraction of the leaves covered by intercepted rain or dew (δ) increases. The impact of soil moisture on T_{2m} and H_{2m} follows similar guidelines. Since there is only one "free" layer in ISBA and the superficial soil moisture corresponds to a very small depth of 1 cm, evaporation is essentially controlled by the mean soil moisture. Here, ω_p is expected to reflect the short-term variations of the latent heat fluxes at the land surface as well as the smooth evolution of moisture deeper in the soil. This makes comparisons to the few available soil moisture observations intrinsically difficult. The problem is of course enhanced in the framework of a global NWP model with a relatively coarse resolution.

4. Analysis of soil variables

The operational ARPEGE suite uses a 6-h assimilation cycle; that is, the model fields are updated every 6 h using observations. Ninety-six- and 72-h forecasts with a shorter cutoff analysis are run twice a day, at 0000 and 1200 UTC, respectively, starting from the assimilation suite. The physical package used in the forecast is described in Geleyn et al. (1995), and the dynamical part, especially its features related to variable resolution, in Yessad and Bénard (1996). Initialization uses an incremental digital filtering technique (Lynch et al. 1997). Analysis is performed in four successive stages, beginning with the quality control of observations, based on the OI analysis code for ARPEGE. Upper air fields are analyzed afterward using an incremental 3D variational approach (Thépaut et al. 1998). The next step, called *surface analysis*, is a univariate OI analysis of screen-level fields T_{2m}, H_{2m}, and 10-m wind, using TEMP and SYNOP/SHIP observations. Finally soil temperature and moisture are corrected, following the methods described by Coiffier et al. (1987) for T_s, T_p and Mahfouf (1991) for ω_s, ω_p. Both are based on optimal interpolation from 2-m observations of temperature and relative humidity. Since the geographical distribution of observed data and the model grid usually differ, the gridded fields issued from surface analysis are used as an approximation of observed values.

Surface and mean soil temperature analyses hardly differ from Coiffier et al. (1987) and are quite simple:

$$\Delta T_s = \Delta T_{2m} \qquad \Delta T_p = \frac{\Delta T_{2m}}{2\pi}, \tag{17}$$

where Δ stands for the analysis increment, that is, analyzed minus predicted values at each grid point. Variations of the mean soil temperature are damped in the analysis as in the forecast processes. Corrections for both T_s and T_p are performed in any case. Assimilation experiments with full or partial switch off of temperature analysis have shown a clear deterioration of forecasts (Giard and Bazile 1997a). As an example, Fig. 3 presents the impact on 6-h forecasts of T_{2m} of a strong damping of temperature corrections by a function of the snow cover fraction (to take into account the lower correlation between 2-m temperature and soil temperature

in the presence of snow). Switching off the analysis of soil temperature and, to a lesser extent, damping the corresponding corrections leads to poor results. The impact on H_{2m} is indeed very small in this case.

Analysis of soil moisture is now based on Mahfouf (1991) using informations from both T_{2m} and H_{2m} observations:

$$\Delta\omega_s = \alpha_s^T \Delta T_{2m} + \alpha_s^H \Delta H_{2m}$$
$$\Delta\omega_p = \alpha_p^T \Delta T_{2m} + \alpha_p^H \Delta H_{2m}. \quad (18)$$

Analysis of superficial soil moisture (and maybe also of surface temperature) could be suppressed, since the corresponding information is very quickly lost during the forecast, but has been kept for now. Neither W_l nor W_f are analyzed. The coefficients[1] $\alpha_{s/p}^{T/H}$ depend on soil texture, increasing as the standard range of variation of soil moisture $\delta\omega = \omega_{\rm fc} - \omega_{\rm wilt}$ (as suggested by F. Bouttier 1994, personal communication), on local solar time t^*, on cloudiness (Cl), and on vegetation characteristics. The following analytical formulation is retained (Giard and Bazile 1996), which avoids some problems encountered with the formulation of Bouttier et al. (1993a):

$$\alpha_s^{T/H} = \frac{\delta\omega}{\delta\omega_r} B(\mathrm{Cl})(1 - \mathrm{veg}) \times [a_0^{T/H}(t^*) + a_1^{T/H}(t^*)\mathrm{veg} + a_2^{T/H}(t^*)\mathrm{veg}^2] \quad (19)$$

$$\alpha_p^{T/H} = \frac{\delta\omega}{\delta\omega_r} B(\mathrm{Cl}) \times \left\{ (1 - \mathrm{veg})[b_0^{T/H}(t^*) + b_1^{T/H}(t^*)\mathrm{veg} + b_2^{T/H}(t^*)\mathrm{veg}^2] + \mathrm{veg}\frac{\mathrm{LAI}}{R_{\rm sm}}[c_0^{T/H}(t^*) + c_1^{T/H}(t^*)\mathrm{veg}] \right\}; \quad (20)$$

$\delta\omega_r$ is a reference value for $\delta\omega$, corresponding to loam. The local solar time t^*, expressed in hours, is a straightforward integer function of declination and absolute solar time (i.e., of date, latitude, and longitude). It is scaled according to the length of daylight, so that it is equal to 6 at dawn, 12 at midday, 18 at twilight, and 24 at midnight whenever possible. Also, B represents a simple potential weighting by the mean cloudiness over the past 6 h: $B(\mathrm{Cl}) = 1 - B_1\mathrm{Cl}^{B_2}$, where B_1 and B_2 are tunable parameters.

The dependency on veg, LAI, and $R_{\rm sm}$ is consistent with the ISBA equations and tries to avoid spurious corrections of soil moisture with regard to vegetation characteristics. The polynomial terms $a_n^{T/H}(t^*)$, $b_n^{T/H}(t^*)$, $c_n^{T/H}(t^*)$ were derived from the available set of OI coefficients ($\tilde{\alpha}_{s/p}^{T/H}$) computed by Mahfouf (1991), and described in Bouttier et al. (1993a) or Giard and Bazile (1996), for loam and a few vegetation characteristics for each value of t^*. A new computation of statistics using the current version of the model and other fields, such as radiation fluxes, had to be postponed because of workplan constraints. To begin with, the functions are adjusted for each value of the local solar time so as to best fit the original OI coefficients. First, $a_n^{T/H}$ (n = 0, 1, 2) are computed from 10 experiments with veg ranging from 0.0 to 0.9, while LAI/$R_{\rm sm}$ remains constant (LAI = 1 m^2 m^{-2}, $R_{\rm sm}$ = 40 s m^{-1}), by minimizing the cost function:

$$\sum_{i=0}^{9} (1 - \mathrm{veg}_i)\{\tilde{\alpha}_{si}^{T/H} - (1 - \mathrm{veg}_i) \times [a_0^{T/H} + a_1^{T/H}(t)\mathrm{veg}_i + a_2^{T/H}(t)\mathrm{veg}_i^2]\}^2,$$
$$\mathrm{veg}_i = \frac{i}{10}; \quad (21)$$

$c_n^{T/H}$ (n = 0, 1) are then computed in two steps. First $c_0^{T/H} + 0.5c_1^{T/H}$ is obtained from the four experiments testing the impact of minimum surface resistance: veg and LAI are kept constant, equal to 0.5 and 1 m^2 m^{-2}, respectively, while $R_{\rm sm}$ follows a geometric series (40, 80, 160, 320 s m^{-1}). The condition $\tilde{\alpha}_p^{T/H}$ = LAI $R_{\rm sm}^{-1}(c_0^{T/H} + c_1^{T/H})$ applied to a last experiment (veg = 1, LAI = 1 m^2 m^{-2}, $R_{\rm sm}$ = 40 s m^{-1}) provides the additional information. To end with, $b_n^{T/H}$ (n = 0, 1, 2) are computed in a similar way as $a_n^{T/H}$, from $\tilde{\alpha}_p^{T/H}$ − veg LAI $R_{\rm sm}^{-1}(c_0^{T/H} + \mathrm{veg}c_1^{T/H})$. Figure 4 shows the variations of the initial and fitted OI coefficients with the vegetation cover for some characteristic values of t^*, before any further adjustment. A reasonable agreement is obtained,

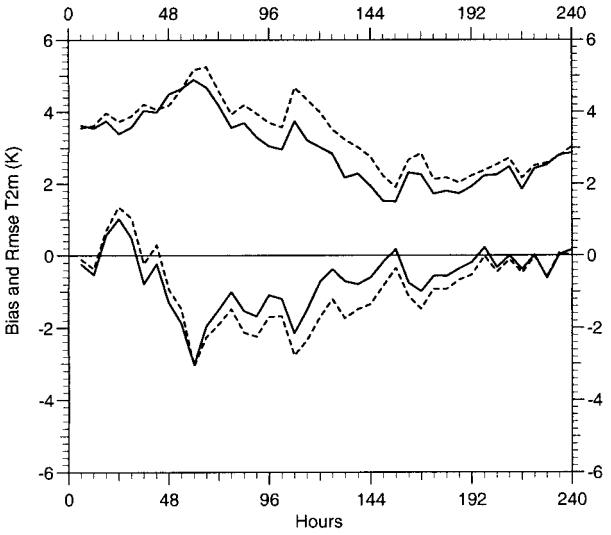

FIG. 3. Difference between predicted and observed T_{2m} (mean and rms errors) during 10-day long assimilation experiments from 2 Jan 1995, over Scandinavia. Full line: analysis of T_s, T_p in any case. Dotted line: no analysis of T_s, T_p in the presence of snow.

[1] The notation $\alpha_{s/p}^{T/H}$ is shorthand for α_s^T, α_p^T, α_s^H, and α_p^H. When used in an equation [e.g., Eq. (19)], the notation implies that the equation represents a set of equations.

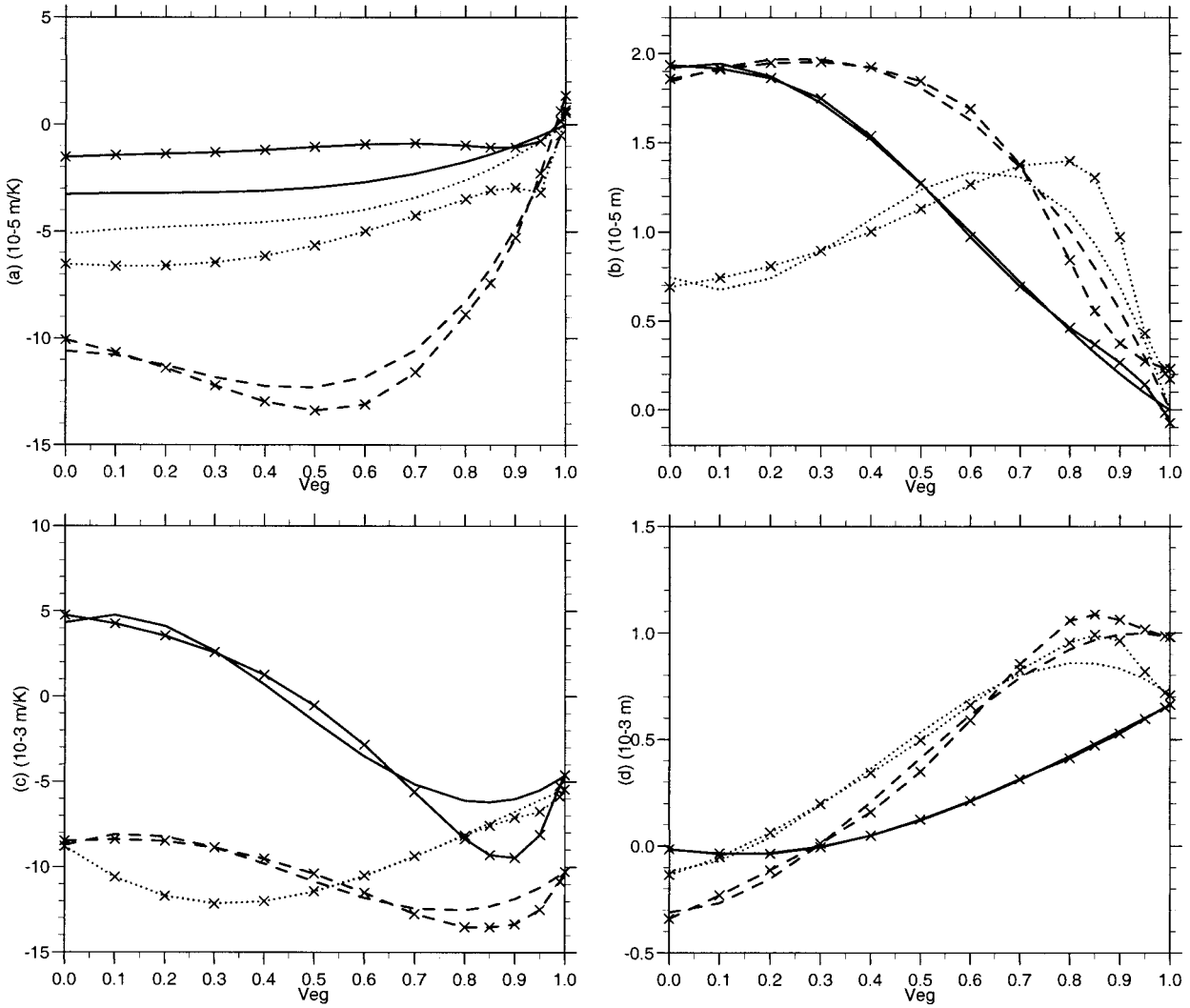

FIG. 4. Variations of the original and fitted OI coefficients with the fraction of the vegetation cover over loam, with LAI = 1 m^2 m^{-2}, R_{sm} = 40 s m^{-1}: (a) α_s^T, (b) α_s^H, (c) α_p^T, (d) α_p^H. Full line t^* = 06, dashed line t^* = 12, dotted line t^* = 18. Crosses refer to the original coefficients.

especially for α_p^T and α_p^H, which are the most important ones.

Afterward a second fit is applied, to each polynomial term, to correct the dependency on t^*. Original OI coefficients have been obtained from 24-h forecasts starting at midnight, so that the range of forecast increases as the local solar time changes and has a nonnegligible impact on statistics, at least beyond $t^* = 18$. This is likely to explain the large discontinuity in the diurnal cycle around midnight or the nonnegligible values of $\tilde{\alpha}_s^{T/H}$ for veg ≈ 1, for instance. Considering that

- original values beyond $t^* = 18$ are probably not reliable for this application;
- values during daytime are most important, since analysis of soil moisture is often switched off during night; and
- it is more careful to underestimate rather than to overestimate corrections;

a simple sinusoidal function of the local solar time with period 24 h has been adjusted to each polynomial term, using values from $t^* = 6$ to $t^* = 18$ for the fit:

$$x(t^*) = x_s \sin(2\pi t^*/24) + x_c \cos(2\pi t^*/24) + x_m \quad \text{(where } x = a_n^{T/H}, b_n^{T/H}, \text{ or } c_n^{T/H}\text{)}. \tag{22}$$

The corresponding sine, cosine, and constant parts are given in Table 2 for each of the 16 polynomial terms.

The last step is, of course, the calibration of OI coefficients since dimensions differ between Mahfouf (1991) and Eq. (18). Note that H_{2m} lies in the range [0, 1] here. An additional set of sensitivity studies has been performed for a wide range of situations and veg-

TABLE 2. Time decomposition of polynomial terms.

x	a_0^T	a_1^T	a_2^T	b_0^T	b_1^T	b_2^T	c_0^T	c_1^T
x_m	−4.1835	−2.6254	−7.1568	−5.9454	−17.3010	−4.0040	11.8959	−294.7318
x_c	6.4087	7.8409	27.9724	5.0276	−18.8650	18.8516	251.5309	−88.1327
x_s	0.9216	−0.0226	1.9319	−0.2597	2.5193	−11.1061	365.3705	−475.6089
x	a_0^H	a_1^H	a_2^H	b_0^H	b_1^H	b_2^H	c_0^H	c_1^H
x_m	1.2045	0.3416	4.1948	−0.0852	−0.1321	1.4457	3.4071	33.1602
x_c	−0.4206	−1.3844	0.6096	0.2169	1.1455	−2.6487	−24.4744	18.8944
x_s	0.5538	1.3866	−4.6419	0.0871	0.4215	−0.7294	−16.4809	26.8836

etation characteristics, with the 1D version of ARPEGE. They have shown a reasonable agreement between the response of the 6-h forecast of 2-m fields to changes in the initial values of ω_s, ω_p and the final values of $\alpha_{s/p}^{T/H}$.

Assimilation experiments trying to assess the impact of such a soil moisture analysis have shown that it is beneficial provided that ω_s and ω_p are effectively responsible for errors on T_{2m} and H_{2m}. In many cases, forecast errors at screen level are not related to soil moisture, whatever the accuracy of the surface scheme. As a consequence additional precautions must be taken to avoid spurious modifications and to keep a realistic soil moisture.

First of all, the analysis is switched off in cases when it clearly has hardly any impact on 2-m fields: very short length of daylight, ice or snow cover, dew, significant precipitation, or strong low-level wind. The second set of constraints concerns soil moisture increments ($\Delta\omega_s$, $\Delta\omega_p$). Analysis is not allowed to make ω_p/ω_s jump outside the range [vegω_{wilt}, ω_{fc}]/[0, ω_{fc}], where vegω_{wilt} is a compromise between 0, for bare ground, and ω_{wilt} for vegetation. Whenever the predicted value is already outside this interval, increments are limited so that they can only tend to restore reasonable values. Another modification is related to the strong diurnal cycle that may appear in the forecast error on T_{2m} and H_{2m}, as in Figs. 1 or 6. It may be caused by an incorrect initialization of ω_p but is often due to other problems, for instance an inaccurate description of vegetation as in Fig. 1, inappropriate tunings in physics, or shortcomings in the surface analysis. Directly applying Eq. (18) in such a case leads to strong diurnal oscillations of soil moisture and thus an enhanced diurnal cycle of H_{2m} (and to a lesser extent T_{2m}) errors, as shown in Fig. 6. This problem was also met with the former surface and analysis schemes in ARPEGE. The solution here is to smooth corrections of the mean soil moisture using a history file. Thus, ω_p is changed by the mean of the last four analysis increments, that is, the mean increment over the past 24 h. The superficial soil moisture (ω_s) is not smoothed, since corrections are smaller and have less impact. This has proved quite successful. On the other hand, a tuning of the damping by cloudiness was postponed, since it appears less important than the modifications described here [i.e., B(Cl) was set to 1 in Eqs. (19) and (20)].

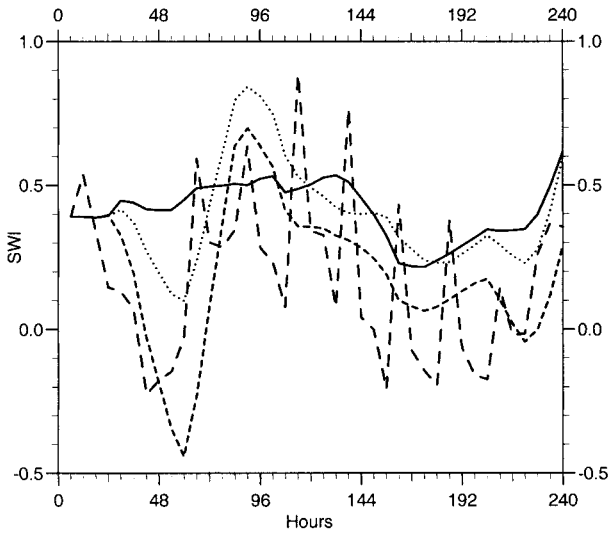

FIG. 5. Evolution of SWI during 10-day long assimilation experiments from 2 Jul 1995, over France (44°N, 2°W; 50°N, 8°E). Large dashed line: initial ISBA scheme + loose threshold on precipitation (6 mm/6 h) for soil moisture analysis. Dashed line: initial ISBA scheme + loose threshold on precipitation + smoothing of ω_p increments. Dotted line: modified ISBA scheme + loose threshold on precipitation + smoothing of ω_p increments. Full line: modified ISBA scheme + strict threshold on precipitation (0.6 mm/6 h) + smoothing of ω_p increments.

Figures 5 and 6 show the impact over France, for 10-day long assimilation experiments for a summer situation, of four successive improvements in analysis or forecast:

- smoothing of ω_p corrections,
- some refinements in ISBA—stronger limitation of C_t (from 10×10^{-6} to 8×10^{-6} K m^2 J^{-1}) and smaller ratio of thermal to dynamical roughness length over land (from 1 to 0.1), and
- reduction of the threshold on precipitation over the past 6 h (from 6 mm/6 h to 0.6 mm/6 h) for switching off soil moisture analysis.

At each step, the evolution of the soil wetness index [SWI = $(\omega_p - \omega_{\text{wilt}})/(\omega_{\text{fc}} - \omega_{\text{wilt}})$] gets more reasonable (Fig. 5), with the suppression of spurious variations of large amplitude, while the forecast of T_{2m} and particularly H_{2m} (Fig. 6) keeps improving. The overall gain from these modifications is remarkable. Strong diurnal

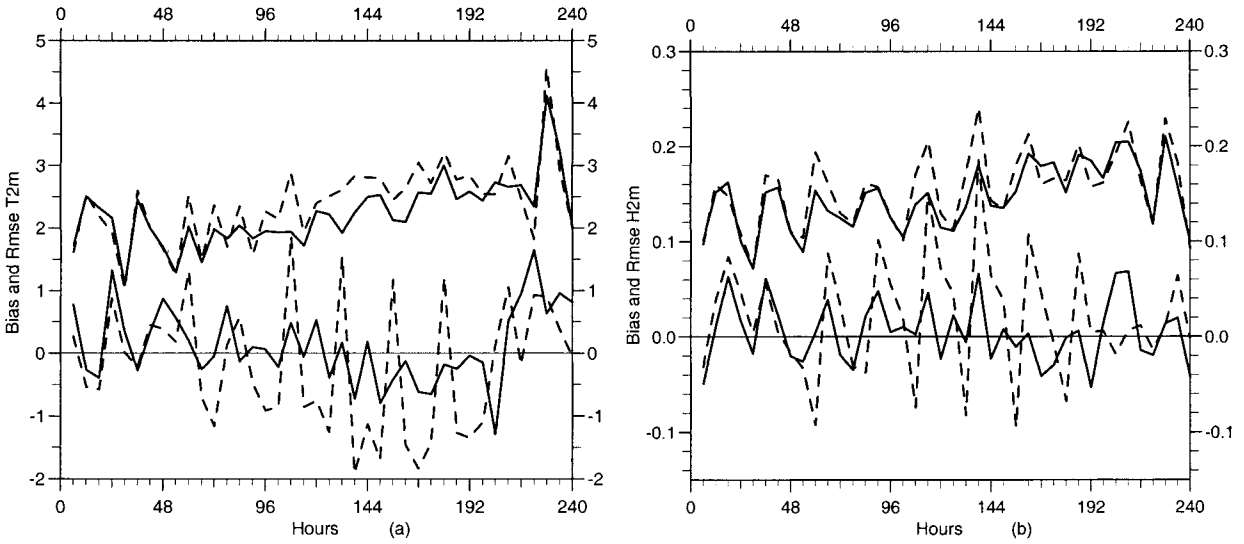

FIG. 6. Difference between predicted and observed values for (a) T_{2m} and (b) H_{2m} (mean and rms errors) over France (44°N, 2°W; 50°N, 8°E) for similar conditions as in Fig. 5. Notations are the same but only the first and the last experiments are shown.

oscillations have been damped, and the rms errors on T_{2m} and H_{2m} are reduced by up to 1 K and 0.05 in this test case.

Whereas H_{2m} is usually very sensitive to soil moisture, T_{2m} often exhibits long-term biases related to very different problems (e.g., radiative forcing errors). In this case, using the full amount of information from the T_{2m} analysis increment (ΔT_{2m}) may cause severe undue changes in the soil water content with hardly any positive feedback (or even a negative one) on the atmosphere. For instance, Fig. 7 shows the results of two 10-day long assimilation experiments for a winter situation over Spain. Figure 7a exhibits a clear cold bias for T_{2m}, while H_{2m} keeps close to observations (Fig. 7b) for both cases. Without any further precautions, the soil undergoes a drastic drying (Fig 7c), limited to $\omega_p \geq$ veg ω_{wilt} by the previous constraints but quite unrealistic for this season. Furthermore this does not help with reducing the errors in 2-m fields. To avoid such problems, a *systematic long term* T_{2m} increment ($\Delta^* T_{2m}$) is computed recursively and updated at each analysis step (i.e., every 6 h) as $\Delta^* T_{2m} = (1 - r)\Delta^* T_{2m} + r\Delta T_{2m}$, using a history file. Only the deviation from this mean value, that is, $\Delta T_{2m} - \Delta^* T_{2m}$, is used as input for the correction of ω_s and ω_p. Of course, this does not apply to the analyses of T_s and T_p. The weight r has been set to 0.5, so that the elimination of large biases on T_{2m} begins to be effective after 2 or 3 days. This avoids large drifts in soil moisture without involving any significant deterioration in the forecast, as illustrated by Fig. 7. The distance to T_{2m} observations is sometimes slightly enhanced, but errors in H_{2m} are reduced.

Finally, the mean soil temperature and moisture are slightly restored toward climatology after the analysis step, like in the former scheme. This aims to prevent large drifts in the case where no observations are available over a large domain or a long period. The corresponding timescales are about 10 days for T_p and 100 days for ω_p.

5. Results and conclusions

The successive modifications described above were tested for 10-day long assimilation experiments and 72-h forecasts with spectral truncation T119*c*3.5, over a summer and a winter situation (July 1995, January 1995). The evolution of soil and surface variables and the fit to T_{2m} and H_{2m} observations were controlled, focusing on six large homogeneous domains covering a large range of vegetation characteristics and climates, from equatorial Africa to Scandinavia. The whole ISBA package, including changes in the physics, the analysis, and the land surface description, was put through more extensive validation tests afterward.

First, to check the long-term behavior, a 1-yr long assimilation experiment, covering 1997, was performed with a low model resolution (T79, without stretching). The corresponding annual cycle of soil temperature, soil moisture, and snow cover looks reasonable, while forecasts keep close to observations. As an example, Fig. 8 shows the evolution of the mean soil temperature and of the soil wetness index for equatorial Africa and Australia. The main features of the corresponding climates are preserved. No large-scale drift is noticed, starting and ending values (one year later) remain close to one another. This experiment has also been used to obtain a first approximation of the climatological surface fields required by the model, since the previous ones were neither consistent with ISBA nor with the new land surface description.

A very thorough checking, at the current operational

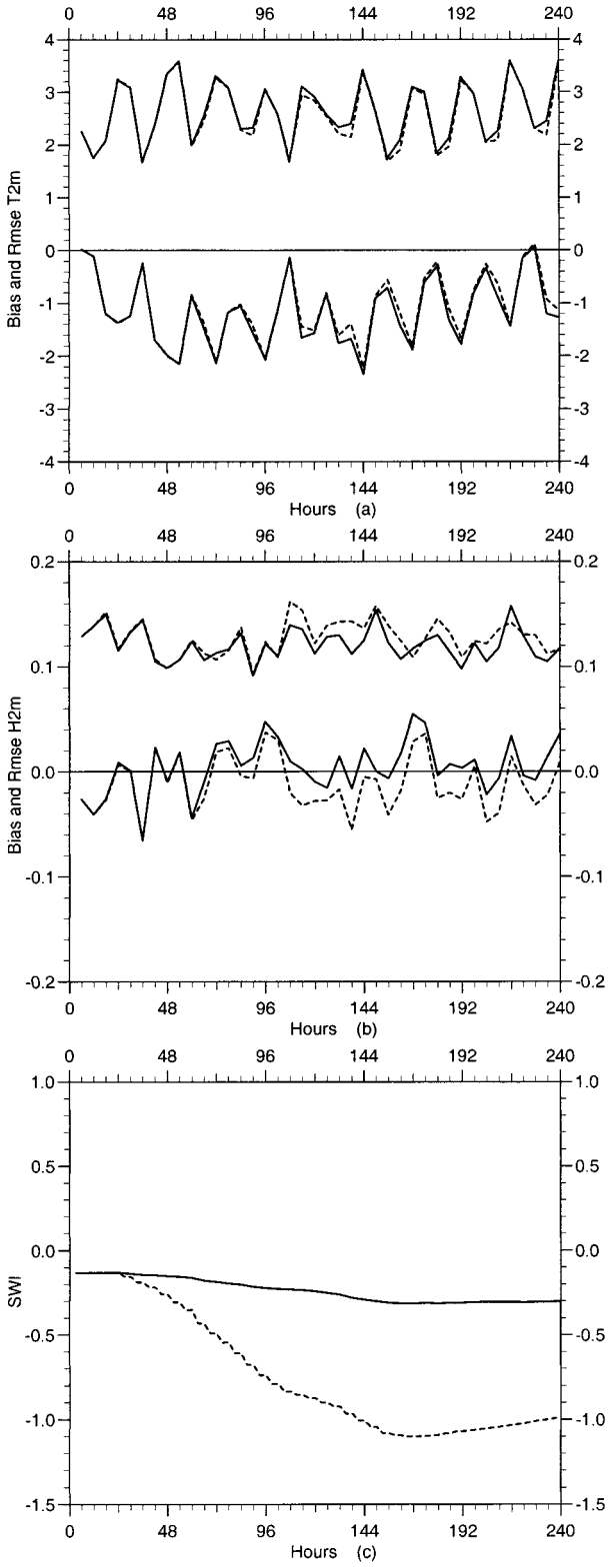

FIG. 7. Difference between predicted and observed values for (a) T_{2m} and (b) H_{2m} (mean and rms errors) and evolution of (c) SWI during 10-day long assimilation experiments from 2 Jan 1995, over Spain (36°N, 10°W; 44°N, 0°). Without (dashed line) and with (full line) elimination of systematic errors on T_{2m}.

resolution (T149*c*3.5), was undertaken afterward. Here an assimilation suite and daily 72-h forecasts, the *parallel suite*, are run for a few weeks under the same conditions as the operational ARPEGE suite, the latter still including the old surface package. The forecasts (6–72 h) issued from the two suites are carefully compared: to analyzed fields, to observations (TEMP, SYNOP), and to other models, considering upper air as well as surface variables. Diagnostics are calculated over domains ranging from small European countries to a hemisphere, covering the whole globe. Two parallel suites were run, from 25 September 1997 to 14 October 1997 and from 17 February 1998 to 16 March 1998, so that a large range of situations were simulated. Upper air scores proved neutral, while a real improvement was noticed near the surface, at the global as well as at the local scale. Figures 9 and 10 show the difference between predicted and observed (SYNOP) values of T_{2m} and H_{2m} along the 11 last 72-h forecasts of the autumn parallel and operational suites, over France and Norway, respectively. Only stations from the European Working Group on Limited Area Modelling (EWGLAM) verification list are used here. Over France, where warm anticyclonic situations dominate, the improvement is quite significant. Biases and rms errors are reduced and the amplitude of the diurnal cycle on H_{2m} errors is damped by a factor 2. The forecast of H_{2m} is slightly improved over Norway but, as nights became colder, a negative bias in temperature appears. At that time the soil water freezing parameterization had not yet been introduced, which is likely to explain such problems. Figures 11 and 12 show the corresponding scores for the winter suites, with the full ISBA modification set. Though temperatures are colder than in October, there is no longer any bias on T_{2m} over Norway, and the rms error is also significantly reduced. The new parameterization of soil water freezing appears quite efficient. The scores on H_{2m} are also improved, with a reduction of the wet bias and a better description of the diurnal cycle. On the other hand, even if the mean error on H_{2m} approaches 0, the gain over France is less significant for this disturbed weather regime, when near-surface fields are driven by upper air flow rather than by surface exchanges. Despite such contrasted situations, an overall improvement in the comparison to SYNOP observations was noticed, as illustrated for the winter suites by Figs. 13 and 14 presenting 2-m scores for some larger domains: north of 20°, Tropics [i.e., (−20°, 20°)], Antarctica.

The forecast of precipitation amount over Europe with the parallel suite was similar to the operational one. For other observations, results were neutral if not better with the ISBA package. Global balances were also examined. The differences between 6-h forecasts and the corresponding analyses, averaged over all the model grid points (i.e., a global mean), were accumulated along the operational and the parallel assimilation suites. When averaged over a long period, this 6-h trend must nearly vanish if the model is well balanced with

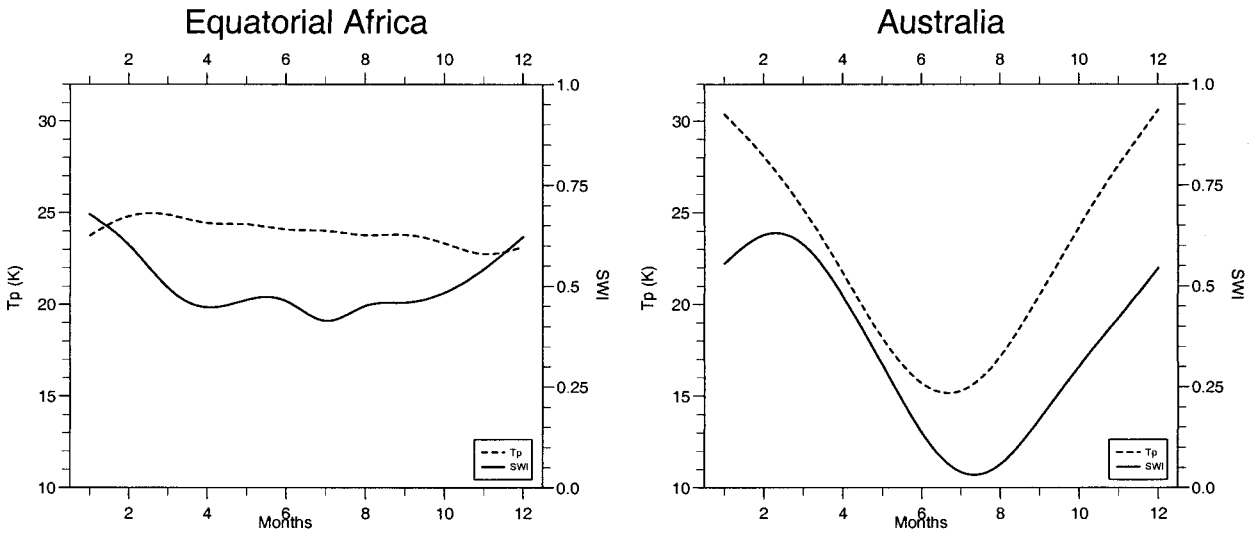

FIG. 8. Evolution of soil wetness index and T_p during a 1-yr long assimilation experiment covering 1997, over equatorial Africa and Australia. Full line: SWI. Dotted line: T_p.

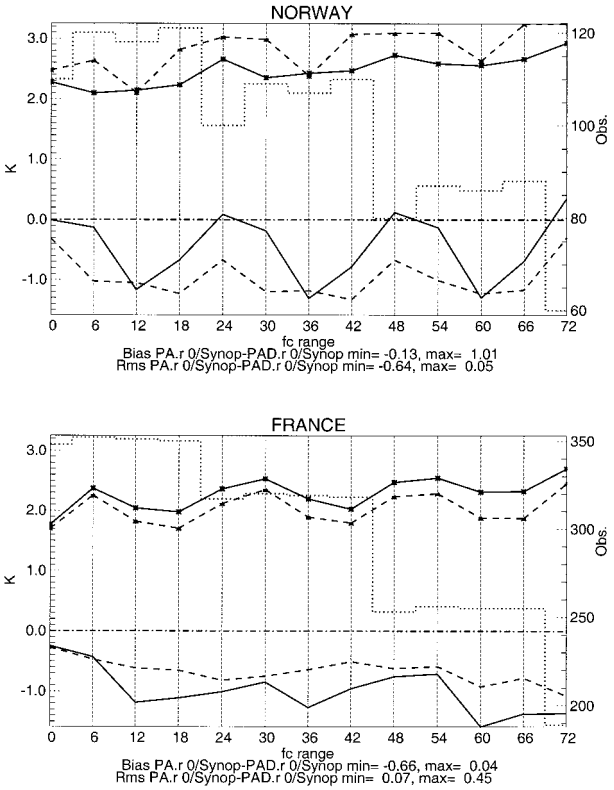

FIG. 9. Difference between predicted and observed value for T_{2m} (mean and rms errors), averaged along 11 72-h forecasts over Norway and France during the autumn parallel suite. Full line: old scheme. Dashed line: ISBA. Dotted line: number of observations used in the comparison.

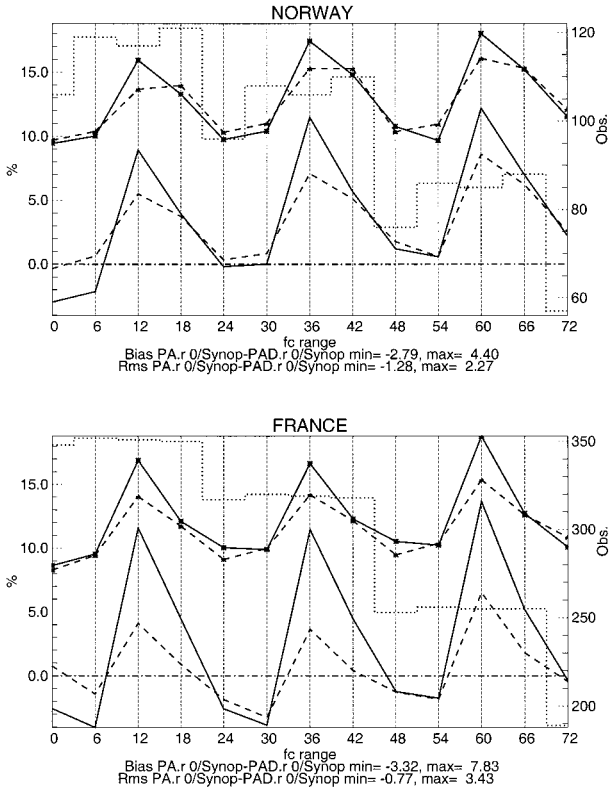

FIG. 10. Difference between predicted and observed value for H_{2m} (mean and rms errors), averaged along 11 72-h forecasts over Norway and France during the autumn parallel suite. Full line: old scheme. Dashed line: ISBA. Dotted line: number of observations used in the comparison.

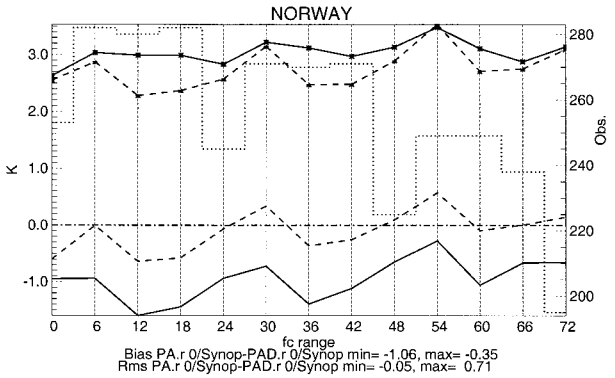

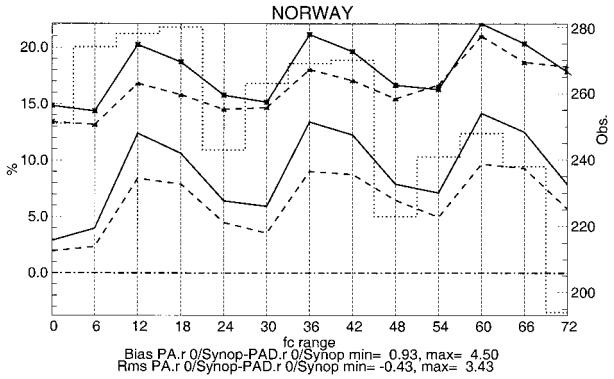

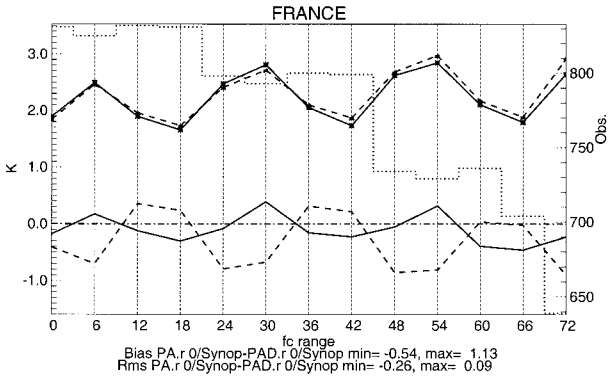

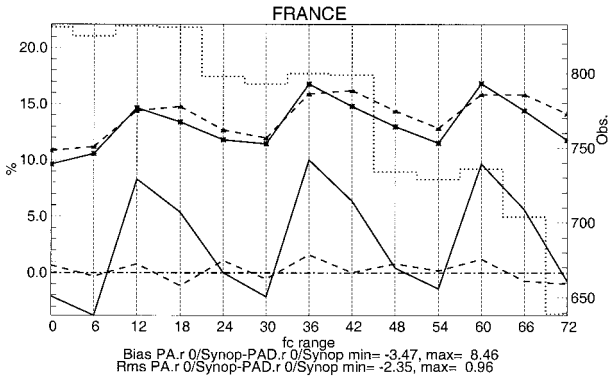

FIG. 11. Difference between predicted and observed value for T_{2m} (mean and rms errors), averaged along 20 72-h forecasts over Norway and France during the winter parallel suite. Full line: old scheme. Dashed line: ISBA. Dotted line: number of observations used in the comparison.

FIG. 12. Difference between predicted and observed value for H_{2m} (mean and rms errors), averaged along 20 72-h forecasts over Norway and France during the winter parallel suite. Full line: old scheme. Dashed line: ISBA. Dotted line: number of observations used in the comparison.

its own analysis. Large values point out deficiencies of the set of physical parameterizations. Figure 15 shows the corresponding average vertical profiles for temperature and specific humidity for the autumn and winter comparisons. The ISBA assimilation cycle is better balanced than the operational one, especially for specific humidity (Fig. 15b). In the operational assimilation cycle the global mean evaporation, 3 mm day^{-1}, was too large when compared to the climatological value: $\approx$2.7 mm day^{-1}. With the ISBA package we reduce the surface evaporation by about 0.15 mm day^{-1}.

Finally, as a check at the local scale, the daily forecasts from both the parallel and the operational suites were compared to observations from the Monitoring the Usable Soil Reservoir Experimentally (MUREX) field experiment (Calvet et al. 1998) for the two intensive validation periods. Figure 16 shows the mean diurnal cycle of T_{2m} and H_{2m} over the last 6 days of the autumn suites, for observations and 24-h forecats at the nearest model grid point. Time sampling is 0.5 h for observations (which are not used in the assimilation) and 3 h for model output, and no further adjustment is applied apart from a height correction for T_{2m}. The ISBA package is also better in this case, particularly for H_{2m}, and in reasonable agreement with observations in spite of large handicaps inherent to such a test. Accordingly, the forecast of latent heat fluxes is improved, with an average of 48 W m^{-2} over 24 h for the parallel suite, to be compared to 45 W m^{-2} for observations and 73 W m^{-2} for the operational suite.

As a consequence, the whole ISBA modification set became operational on 16 March 1998, simultaneously in the global ARPEGE model and in the seven operational ALADIN models—Albachir (in Morocco), Belgium, France, Hungary, Limited Area Model for Central Europe (LACE), Romania, and Slovenia—and has proved satisfying since then. The strength and also the pioneering aspect of this modification was that its three facets (forecast, analysis, and databases) have been considered simultaneously and have received equal consideration. None of them ought to be neglected in such a context.

However, some additional refinements are already considered. First, the high-resolution vegetation database has been extended northward and eastward over Europe in October 1998. New datasets will be introduced whenever available. ''Predicted'' values of T_{2m} and H_{2m} are now updated just after upper air analysis, which enables the further reduction of the impact of upper air forecast errors on soil moisture corrections. Stricter constraints on soil moisture analysis will be tested, in order to damp some remaining unexpected var-

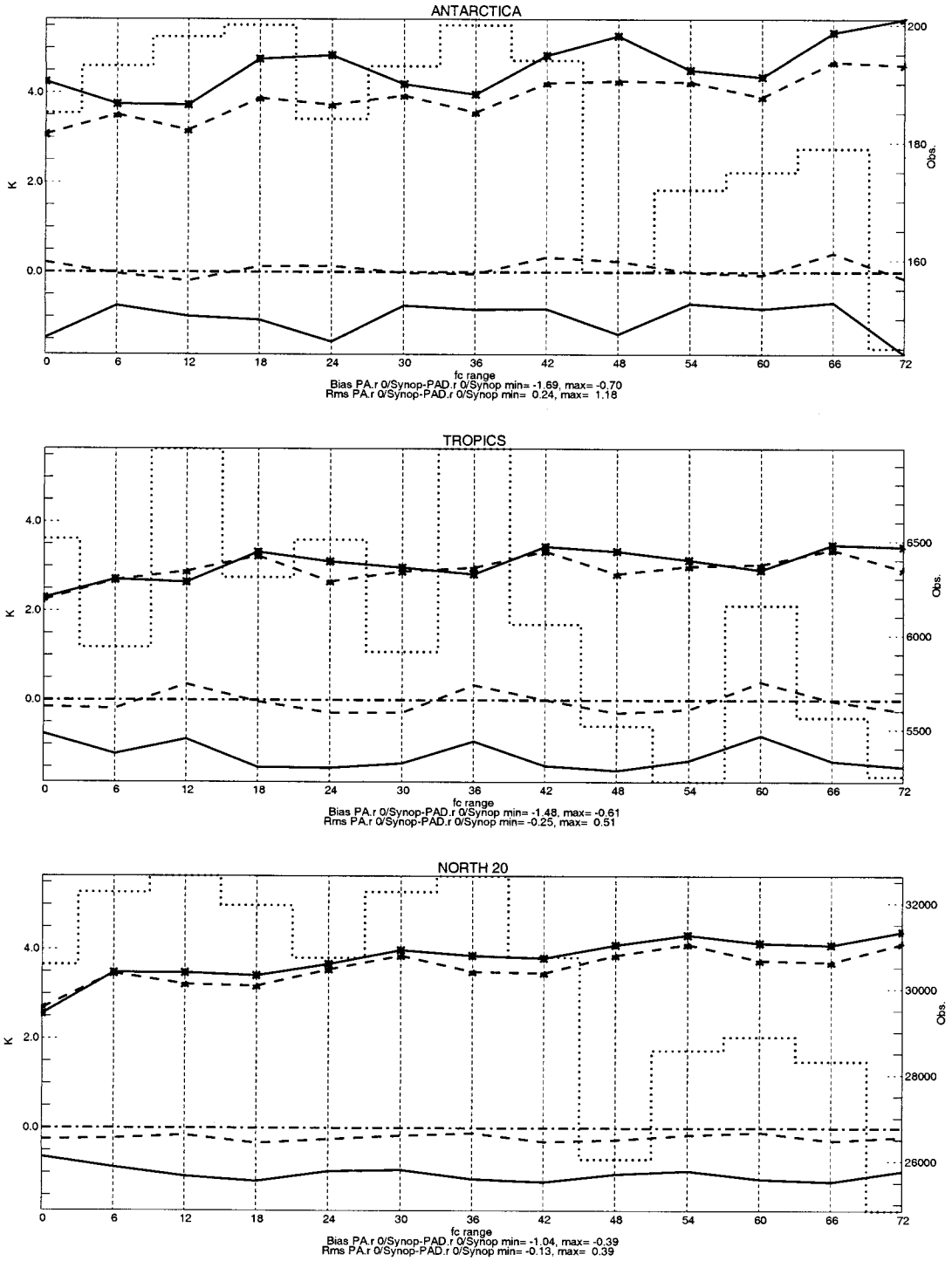

FIG. 13. Difference between predicted and observed value for T_{2m} (mean and rms errors), averaged along 11 72-h forecasts over north of 20°, Tropics, and Antarctica during the winter parallel suite. Full line: old scheme. Dashed line: ISBA. Dotted line: number of observations used in the comparison.

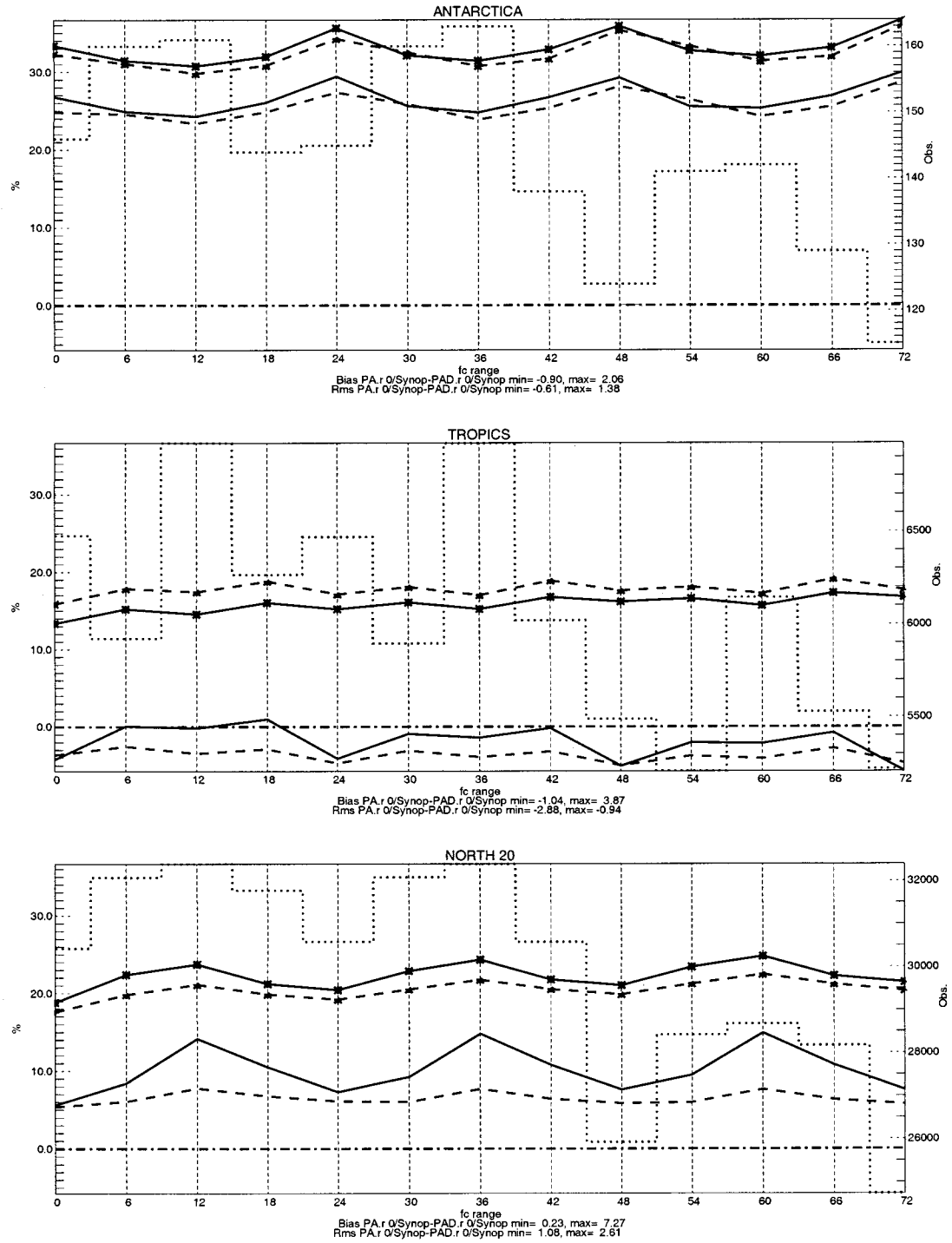

FIG. 14. Difference between predicted and observed value for H_{2m} (mean and rms errors), averaged along 11 72-h forecasts over north of 20°, Tropics, and Antarctica during the winter parallel suite. Full line: old scheme. Dashed line: ISBA. Dotted line: number of observations used in the comparison.

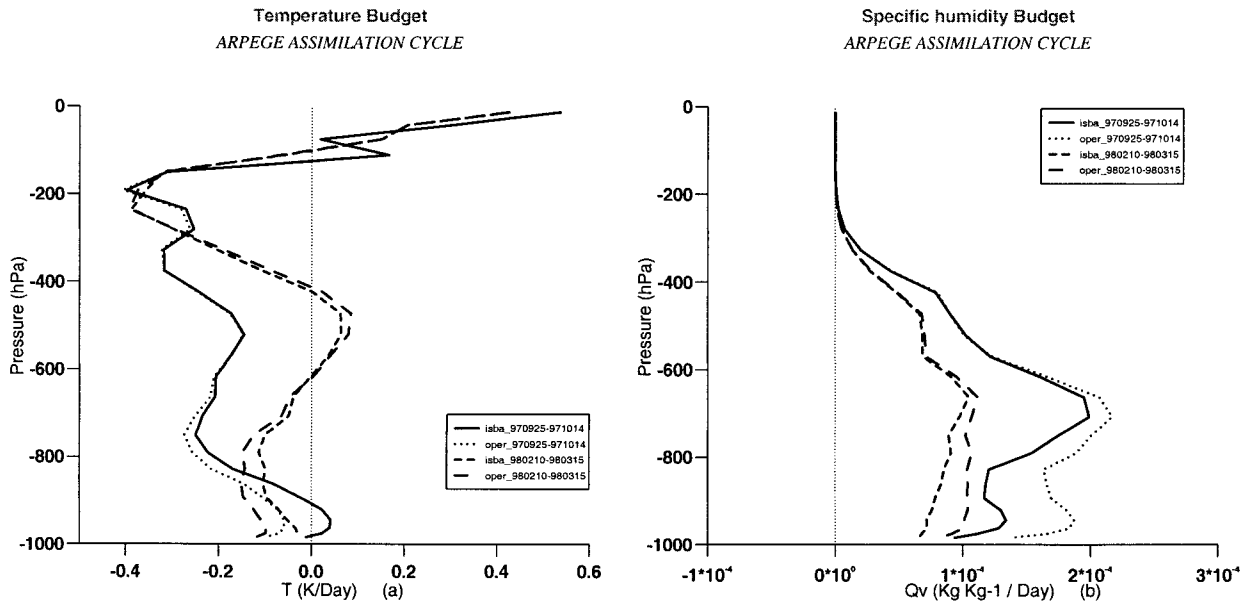

FIG. 15. Horizontal mean of (a) the temperature tendency and (b) the specific humidity tendency for the 6-h forecast of the assimilation cycle. Full line/dotted line (autumn parallel suite): ISBA/old scheme. Dashed line/large dashed line (winter parallel suite): ISBA/old scheme.

iations of SWI. The analysis of superficial soil moisture may be suppressed in the meantime. For ISBA itself, the next change will be the introduction of freezing for the superficial water content too. A further move to several adjacent layers into the soil, coupled with the introduction of a skin temperature, is also considered. However, the efficiency of such improvements will depend on parallel developments in the analysis of 2-m fields or in other parameterization schemes.

Acknowledgments. The authors wish to thank J. Noilhan and H. Douville for many helpful discussions, J.-L. Champeaux for the land cover database, and F. Pouponneau for the graphics of the parallel suites. Our acknowledgments also go to the HIRLAM working group on soil and surface analysis, and to the people responsible for ALADIN operational activities outside Météo-France that accepted the strong constraint of a simultaneous operational move on 16 March 1998.

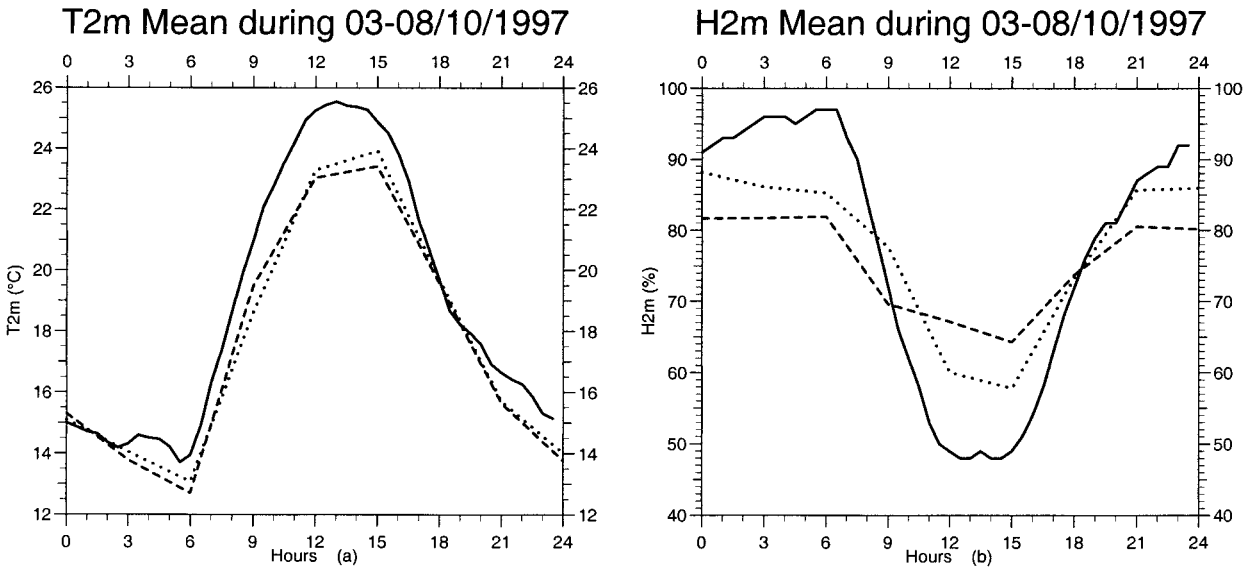

FIG. 16. Mean of six 24-h forecasts at the nearest grid point to the MUREX site: (a) T_{2m}, (b) H_{2m}. Full line: Observations. Dotted line: ISBA. Dashed line: old scheme.

APPENDIX A
Lookup Tables for the Global Land Cover Database

TABLE A1. Leaf area index ($m^2\ m^{-2}$).

Type of vegetation	Jan	Feb	Mar	Apr	May	Jun	Jul	Aug	Sep	Oct	Nov	Dec	Non-varying
Crop	0.1	0.1	0.1	0.5	1.0	2.0	3.0	3.5	4.0	0.1	0.1	0.1	
Short grass													1.0
Evergreen needleaf tree													5.0
Deciduous needleaf tree	0.1	0.1	0.5	1.0	2.0	4.0	5.0	5.0	4.0	2.0	1.0	0.1	
Deciduous broadleaf tree	0.1	0.1	0.5	1.0	2.0	4.0	5.0	5.0	4.0	2.0	1.0	0.1	
Evergreen broadleaf tree													6.0
Savannah	0.5	0.5	0.5	0.5	0.5	0.5	1.0	2.0	2.0	1.5	1.0	1.0	
Tundra	1.0	1.0	0.5	0.1	0.1	0.1	0.1	1.0	2.0	1.5	1.5	1.0	
Semidesert													0.5
Bog or marsh													4.0
Evergreen shrub													3.0
Deciduous shrub	0.5	0.5	1.0	1.0	1.5	2.0	3.0	3.0	2.0	1.5	1.0	0.5	
Mixed wood	3.0	3.0	3.0	4.0	4.5	5.0	5.0	5.0	4.0	3.0	3.0	3.0	

TABLE A2. Vegetation cover.

Type of vegetation	Jan	Feb	Mar	Apr	May	Jun	Jul	Aug	Sep	Oct	Nov	Dec	Non-varying
Crop	0.05	0.05	0.05	0.10	0.20	0.40	0.80	0.80	0.90	0.05	0.05	0.05	
Short grass													0.85
Evergreen needleaf tree													0.90
Deciduous needleaf tree													0.90
Deciduous broadleaf tree													0.90
Evergreen broadleaf tree													0.99
Savannah													0.30
Tundra													0.50
Semidesert													0.10
Bog or marsh													0.60
Evergreen shrub													0.50
Deciduous shrub													0.50
Mixed wood													0.90

TABLE A3. Root depth (d_r), albedo of vegetation (α_v), roughness length of vegetation ($z0_v$), and minimum surface resistance (R_{sm}).

Type of vegetation	d_r (m)	α	$z0_v$ (m)	R_{sm} (m s^{-1})
Crop	2.0	0.20	0.15	40
Short grass	1.5	0.20	0.02	40
Evergreen needleaf tree	3.0	0.10	2.00	250
Deciduous needleaf tree	1.0	0.11	2.00	250
Deciduous broadleaf tree	3.0	0.12	2.00	250
Evergreen broadleaf tree	3.0	0.12	4.00	250
Savannah	2.0	0.20	0.10	40
Tundra	1.0	0.16	0.05	150
Semidesert	1.0	0.25	0.05	150
Bog or marsh	1.0	0.12	0.05	150
Evergreen shrub	2.0	0.20	0.10	150
Deciduous shrub	2.0	0.20	0.10	150
Mixed wood	2.0	0.12	2.00	250

APPENDIX B
Lookup Tables for the Champeaux Land Cover Database

TABLE B1. Leaf area index ($m^2\ m^{-2}$).

Type of vegetation	Jan	Feb	Mar	Apr	May	Jun	Jul	Aug	Sep	Oct	Nov	Dec
Crop (1)	1.0	1.0	1.0	2.0	4.0	4.0	4.0	4.0	3.0	2.0	1.0	1.0
Mediterranean crop	0.5	0.5	0.5	0.5	1.0	1.0	0.5	0.5	0.5	0.5	0.5	0.5
Cereal (1)	0.5	0.5	0.5	2.0	3.0	4.0	4.0	3.0	2.0	1.0	0.5	0.5
Crop (2)	1.0	1.0	1.0	2.0	3.0	3.0	2.0	2.0	2.0	1.0	1.0	1.0
Cereal (2)	0.5	0.5	1.0	2.0	4.0	4.0	3.0	2.0	1.0	1.0	0.5	0.5
Crop and grassland	1.0	1.0	2.0	2.0	3.0	3.0	2.5	2.5	2.0	2.0	1.0	1.0
Pasture land	1.0	1.0	1.0	2.0	3.0	3.0	3.0	3.0	3.0	2.0	1.0	1.0
Crop (3)	1.0	2.0	3.0	3.0	2.0	1.0	1.0	1.0	1.0	1.0	1.0	1.0
Crop (4)	1.0	1.0	2.0	2.0	1.0	1.0	1.0	1.0	1.0	1.0	1.0	1.0
Vineyard	0.5	0.5	0.5	0.5	0.5	0.5	0.5	0.5	0.5	0.5	0.5	0.5
Forest	2.0	2.0	2.0	2.5	3.0	4.0	4.0	4.0	3.0	2.5	2.0	2.0

TABLE B2. Vegetation cover.

Type of vegetation	Jan	Feb	Mar	Apr	May	Jun	Jul	Aug	Sep	Oct	Nov	Dec
Crop (1)	0.45	0.45	0.70	0.91	0.91	0.91	0.91	0.91	0.83	0.70	0.45	0.45
Mediterranean crop	0.26	0.26	0.26	0.26	0.45	0.45	0.26	0.26	0.26	0.26	0.26	0.26
Cereal (1)	0.26	0.26	0.26	0.70	0.83	0.91	0.91	0.83	0.70	0.45	0.26	0.26
Crop (2)	0.45	0.45	0.45	0.70	0.83	0.83	0.70	0.70	0.70	0.45	0.45	0.45
Cereal (2)	0.26	0.26	0.45	0.70	0.91	0.91	0.83	0.70	0.45	0.45	0.26	0.26
Crop and grassland	0.45	0.45	0.70	0.70	0.83	0.83	0.77	0.77	0.70	0.70	0.45	0.45
Pasture land	0.45	0.45	0.45	0.70	0.83	0.83	0.83	0.83	0.83	0.70	0.45	0.45
Crop (3)	0.45	0.45	0.70	0.83	0.83	0.70	0.45	0.45	0.45	0.45	0.45	0.45
Crop (4)	0.45	0.45	0.70	0.70	0.59	0.45	0.45	0.45	0.45	0.45	0.45	0.45
Vineyard	0.30	0.30	0.30	0.30	0.30	0.30	0.30	0.30	0.30	0.30	0.30	0.30
Forest	0.63	0.63	0.63	0.71	0.78	0.87	0.87	0.87	0.78	0.71	0.63	0.63

TABLE B3. Root depth (d_r), albedo of vegetation (α_v), roughness length of vegetation ($z0_v$), and minimum surface resistance (R_{sm}).

Type of vegetation	d_r (m)	α	$z0_v$ (m)	R_{sm} ($m\ s^{-1}$)
Crop (1)	2.0	0.2	0.15	40
Mediterranean crop	2.0	0.2	0.15	80
Cereal (1)	1.5	0.2	0.15	40
Crop (2)	2.0	0.2	0.15	40
Cereal (2)	2.0	0.2	0.15	40
Crop and grassland	2.0	0.2	0.15	40
Pasture land	1.5	0.2	0.15	40
Crop (3)	2.0	0.2	0.15	40
Crop (4)	2.0	0.2	0.15	40
Vineyard	1.0	0.2	0.15	80
Forest	3.0	0.1	2.0	150

APPENDIX C

List of Symbols Not Otherwise Defined in the Text

Maximum intercepted water by the canopy	$W_{l\max}$
Net radiation	R_n
Sensible heat flux	H
Condensation latent heat	L_v
Fusion latent heat	L_f
Bare ground evaporation	E_g
Evaporation from intercepted water	E_l
Transpiration	E_{tr}
Melting of snow	M_s
Melting or freezing of soil water content	F_w
Time constant of one day	τ
Precipitation	P
Runoff from interception water reservoir	R_l
Runoff from surface water reservoir	R_s
Runoff from deep soil water reservoir	R_p
Density of liquid water	ρ
Depth of the superficial layer (1 cm)	d_s
Force–restore coefficients for soil moisture	C_1, C_2
Maximum and minimum for $C_1 d_s^{-1}$	C_{1max}, C_{1sat}
Coefficient for gravitational drainage	C_3
Saturated volumetric water content	ω_{sat}
Field capacity volumetric water content	ω_{fc}
Wilting point volumetric water content	ω_{wilt}
Volumetric water content when gravity balances the capillarity forces	ω_{seq}
Triple point	T_t
Soil/vegetation heat capacity	C_t
Bare soil heat capacity	C_g
Maximum and minimum of C_g	$C_{g_{max}}$, $C_{g_{sat}}$
Ice heat capacity	C_i
Vegetation heat capacity	C_v
Drag coefficient	C_H
Air density at the lowest model level	ρ_a
Wind speed at the lowest model level	V_a
Specific humidity at the lowest model level	q_a
Specific humidity at saturation	q_{sat}
Snow cover fraction	S_n

REFERENCES

Bazile, E., and D. Giard, 1996: Assimilation and sensitivity experiments in the NWP model ARPEGE with ISBA. *HIRLAM/SRNWP Workshop on Soil Processes and Soil/Surface Data Assimilation,* Madrid, Spain, Swedish Meteorological and Hydrological Institute, 73–78.

——, and ——, 1998: The Operational version of ISBA with its own soil moisture assimilation. *HIRLAM Newsl.*, No. 31, 26–30. [Available from HIRLAM 4 Project, % Met Eireann, Glasnevin Hill, Dublin 9, Ireland.]

Bougeault, P., B. Bret, P. Lacarrère, and J. Noilhan, 1991: An experiment with an advanced surface parameterization in a mesobeta-scale model. Part II: The 16 June 1986 simulation. *Mon. Wea. Rev.*, **119,** 2374–2392.

Bouttier, F., J.-F. Mahfouf, and J. Noilhan, 1993a: Sequential assimilation of soil moisture from atmospheric low-level parameters. Part I: Sensitivity and calibration studies. *J. Appl. Meteor.*, **32,** 1335–1351.

——, ——, and ——, 1993b: Sequential assimilation of soil moisture from atmospheric low-level parameters. Part II: Implementation in a mesoscale model. *J. Appl. Meteor.*, **32,** 1352–1364.

Bouyssel, F., V. Cassé, and J. Pailleux, 1998: Variational surface analysis from screen level atmospheric parameters. *HIRLAM 4 Workshop on Variational Analysis in Limited Area Models,* Toulouse, France, HIRLAM 4 Project.

Braud, I., J. Noilhan, P. Bessemoulin, P. Mascart, R. Haverkamp, and M. Vauclin, 1993: Bareground surface heat and water exchanges under dry conditions: Observations and parameterization. *Bound.-Layer Meteor.*, **66,** 173–200.

Callies, U., A. Rhodin, and D. Eppel, 1998: A case study on variational soil moisture analysis from atmospheric observations. *J. Hydrol.*, **212–213,** 95–108.

Calvet, J.-C., J. Noilhan, and P. Bessemoulin, 1998: Retrieving the root-zone soil moisture from surface soil moisture or temperature estimates: A feasibility study based on field measurements. *J. Appl. Meteor.*, **37,** 371–386.

Champeaux, J.-L., and H. Le Gléau, 1995: Vegetation mapping over Europe using NOAA/AVHRR. *The 1995 Meteorological Satellite Data Users Conf.,* Winchester, United Kingdom, EUMETSAT, 139–143.

——, D. Arcos, E. Bazile, D. Giard, J.-P. Goutorbe, F. Habets, J. Noilhan, and J. Roujean, 1999: AVHRR-derived vegetation mapping over western Europe for use in numerical weather prediction models. *Int. J. Remote Sens.*, in press.

Coiffier, J., Y. Ernie, J.-F. Geleyn, J. Clochard, J. Hoffman, and F. Dupont, 1987: The operational hemispheric model at the French Meteorological Service. *J. Meteor. Soc. Japan, Special NWP Symposium Volume,* 337–345.

Courtier, P., and J.-F. Geleyn, 1988: A global numerical weather prediction model with variable resolution: Application to the shallow-water equations. *Quart. J. Roy. Meteor. Soc.*, **114,** 1321–1346.

Cox, P., 1996: An improved land surface scheme for the UKMO Unified Model—Potential impact on dry summer forecast errors. *HIRLAM/SRNWP Workshop on Soil Processes and Soil/Surface Data Assimilation,* Madrid, Spain, Swedish Meteorological and Hydrological Institute, 79–86.

Geleyn, J.-F., and Coauthors, 1995: Atmospheric parametrization schemes in Météo-France's ARPEGE N.W.P. model. *Proceedings of the 1994 ECMWF Seminar on Physical Parametrizations in Numerical Models,* ECMWF, 385–400.

Giard, D., and E. Bazile, 1996: Assimilation of soil temperature and water content with ISBA in ARPEGE: Some new developments and tests. *HIRLAM Newsl.,* No. 24, Swedish Meteorological and Hydrological Institute, 34–42. [Available from SMHI, S-60176 Norrkopping, Sweden.]

——, and ——, 1997a: Recent developments in soil assimilation. *HIRLAM Newsl.,* No. 26, Swedish Meteorological and Hydrological Institute, 10–12. [Available from SMHI, S-60176 Norrkopping, Sweden.]

——, and ——, 1997b: Soil moisture assimilation in a global variable resolution NWP model. Preprints, *13th Conf. on Hydrology,* Long Beach, CA, Amer. Meteor. Soc., 163–166.

Giordani, H., 1993: Description du codage du schéma de surface NP89 aux normes ARPEGE. Premières validations. Note de Centre CNRM/GMME 15, Météo-France, 72 pp.

Habets, F., and Coauthors, 1999: The ISBA surface scheme in a macroscale hydrological model applied to the Hapex-Mobilly area. Part I: Model and data base. *J. Hydrol.*, **217,** 75–96.

Henderson-Sellers, A., A.-J. Pitman, P.-K. Love, P. Irannejad, and T.-H. Chen, 1995: The Project for Intercomparison of Land Surface Parameterization Schemes (PILPS): Phases 2 and 3. *Bull. Amer. Meteor. Soc.*, **76,** 489–503.

Lynch, P., D. Giard, and V. Ivanovici, 1997: Improving the efficiency

of a digital filtering scheme for diabatic initialization. *Mon. Wea. Rev.*, **125,** 1976–1982.

Mahfouf, J.-F., 1991: Analysis of soil moisture from near surface parameters: A feasibility study. *J. Appl. Meteor.*, **30,** 1534–1547.

——, A. Manzi, J. Noilhan, H. Giordani, and M. Déqué, 1995: The land surface scheme ISBA within the Météo-France climate model ARPEGE. Part I: Implementation and preliminary results. *J. Climate,* **8,** 2039–2057.

Manzi, A.-O., and S. Planton, 1994: Implementation of the ISBA parameterization scheme for land surface processes in a GCM: An annual cycle experiment. *J. Hydrol.,* **155,** 355–389.

Members of the ALADIN International Team, 1997: The ALADIN project: Mesoscale modelling seen as a basic tool for weather forecasting and atmospheric research. *WMO Bull.,* **46,** 317–324.

Noilhan, J., and S. Planton, 1989: A simple parameterization of land surface processes for meteorological models. *Mon. Wea. Rev.*, **117,** 536–549.

——, and J.-F. Mahfouf, 1996: The ISBA land surface parameterisation scheme. *Global Planet. Change,* **13,** 145–149.

Sellers, P.-J., and Coauthors, 1996: The ISLSCP initiative I global datasets: Surface boundary conditions and atmospheric forcings for land–atmospheric studies. *Bull. Amer. Meteor. Soc.,* **77,** 1987–2005.

Thépaut, J.-N., and Coauthors, 1998: The operational global data assimilation system at Météo-France. *HIRLAM 4 Workshop on Variational Analysis in Limited Area Models,* Toulouse, France, HIRLAM 4 Project, 25–31.

Urban, B., J. Hoffman, J. Coiffier, and J.-F. Geleyn, 1985: The initialisation and use of prognostic land-surface values in the french operational forecast system. *Proc. ISLSCP Conf.,* Rome, Italy, ESA SP-248, 61–64.

van den Hurk, B., W. Bastiaanssen, H. Pelgrum, and E. van Meigaard, 1997: A new methodology for assimilation of initial soil moisture fields in weather prediction models using Meteosat and NOAA data. *J. Appl. Meteor.,* **36,** 1271–1283.

Viterbo, P., and A. Beljaars, 1995: An improved land surface parameterization scheme in the ECMWF model and its validation. *J. Climate,* **8,** 2716–2748.

——, and P. Courtier, 1995: The importance of soil water for medium-range weather forecasting. Implications for data assimilation. *Proc. WMO Workshop on Imbalances of Slowly Varying Components of Predictable Atmospheric Motions,* Beijing, China, WMO, 121–130.

Webb, R., C. Rosenzweig, and E. Levine, 1991: A global data set of soil particle size properties. NASA Tech. Rep. 4286, NASA GISS, New York, NY, 34 pp.

Wilson, M., and A. Henderson-Sellers, 1985: A global archive of land cover and soils data sets for use in general circulation climate models. *J. Climatol.,* **5,** 119–143.

Yessad, K., and P. Bénard, 1996: Introduction of a local mapping factor in the spectral part of the Météo-France global variable mesh numerical forecast model. *Quart. J. Roy. Meteor. Soc.*, **122,** 1701–1719.